ISSN 1392 - 1207. MECHANIKA. 2012 Volume 18(2): 135-140

Modelling and simulation of strength and damping of the support pillar welded by longitudinal weld

R. Dundulis*, P. Krasauskas, S. Kilikevičius*****

**Kaunas University of Technology, Kęstučio 27, 44312 Kaunas, Lithuania, E-mail: romualdas.dundulis@ktu.lt*
***Kaunas University of Technology, Kęstučio 27, 44312 Kaunas, Lithuania, E-mail: povilas.krasauskas@ktu.lt*
****Kaunas University of Technology, Kęstučio 27, 44312 Kaunas, Lithuania, E-mail: sigitas.kilikevicius@ktu.lt*

crossref http://dx.doi.org/10.5755/j01.mech.18.2.1575

1. Introduction

Design of pipelines usually comprises calculation for plastic strain account both for resistance to tension and to compression along the axial direction of the pipe. Design of welded pipelines with longitudinal welds in tension is related to the failure modelling of plastic collapse or fracture, while compression resistance failure modes are related to buckling of the pipe in vertical or horizontal direction, or combination with these modes, when a pipeline may buckle in local area of the pipe wall.

However, in some fields of industry, such as stowage works, where should be ensured strongly safety assessment, it is important to design constructions, like platforms, which would be withstand heavy static loading and, in emergences situations, to withstand the same bulk, dropped from the predicted height, with the ability to damp it. Because this task is related to the high safety requirements, the design of construction should be performed as accurate as possible. The major objective in designing of such constructions is to maximize its energy absorption of a possible impact.

Recently, the finite element methods are widely used in analysis of structures for impact energy absorption. Energy absorbing structures for automotive industry are analysed most commonly in research papers. Deformation and damage behaviours of aluminium-alloy under crushing loadings applying experimental and numerical methods were investigated in [1]. In order to find more efficient and lighter crush absorber for optimizing the square aluminium extrusion tube and achieving minimum peak crushing force, response surface methodology has been applied. Investigation of the experimental and numerical quasi-static crushing responses of spot-welded structures with pre-crushed trigger, in order to decrease the initial peak force of spot-welded columns under axial loading was presented in [2]. An investigation of energy absorption characteristics of regular polygonal columns and angle elements under dynamic axial compression by using finite element methods was presented in [3].

Recently, much attention is given to the cellular material filled thin-walled structures. The interaction between metal or polymeric cellular material fillers and the supporting structures produces some desirable crushing behaviours and energy absorption properties [4, 5]. The researches show that aluminium-based metal foams have greater performance than other cellular fillers in structures with high energy absorption capacity.

The aim of this work was to model a pillar produced of stainless 321 steel with a diameter of 400 mm, a height of 800 mm and a wall thickness of 5 mm, welded in the longitudinal direction to withstand predictable static compression load. Also to model the behaviour of the pillar, if the pillar with a heavy weight structure mounted on top of it will be dropped from a height of 5 meters.

2. Materials and specimens

It was decided, that such a cross-section pillar will be produced from a stainless ASME 321 steel sheet [6] with the wall thickness of 5 mm and welded using electrodes CT36 [7]. Because the pillar will be manufactured from the sheet as-received, it was decided to take on whole new dimensions of mechanical properties of the steel by means of tensile testing standard specimens (Fig. 1). It is important, because the pillar manufacturing steps comprises sheet bending and welding and the matter of substance is to know how the mechanical properties of the sheet will change after these technological steps.

Table 1
Mechanical properties of as-received material

Material grade	Yield limit $R_{p0.2}$, MPa	Ultimate strength R_m, MPa	Elongation A_5, %
Stainless ASME 321 steel	220-321	520-720	40-50
Weld electrode CT36	294-311	490-595	20-40

In order to examine the influence of these factors (bending and welding) on mechanical properties of the steel and its welded joint, the standard tensile test has been carried out.

Four type of the specimens (Fig. 1) were used: standard flat specimens with cross-section size of 20x5 mm (3 ones, marked as series P), cut off directly from the stainless 321 steel sheet with the wall thickness of 5 mm (Fig. 1, a); tube contoured specimens (3 ones, marked as series T), cut off from the bended sheet to radius of 200 mm (Fig. 1, b); the same dimension flat and tube contoured specimens, containing the longitudinal axial weld, welded by automatic arc-welding machine using electrodes CT36 marked as series PW and TW respectively (Fig. 1, c and d).

3. Tensile test technique and results

The testing was performed on 10 kN capacity low-cycle tension-compression testing machine UME-

10TM with the stress rate of 20 MPa/s and loading rate of 1 mm/min [LST EN 10002-1:2003].

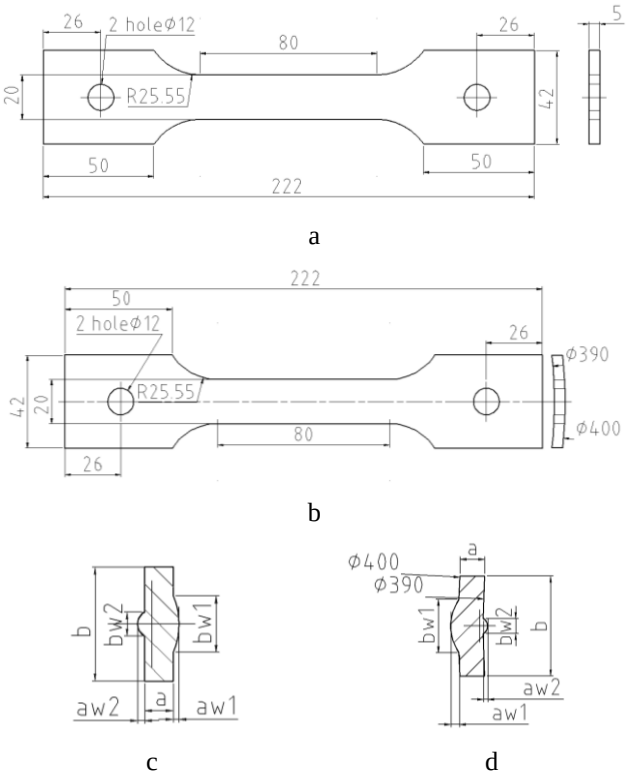

Fig. 1 Shape and measurements of the specimens: a - standard flat specimen (series P); b - tube contoured specimen (series T); c - weld cross-section of the flat specimen (series PW); d - weld cross-section of the tube contoured specimen (series TW)

Cylindrical hardened loading pins with a diameter of 12 mm were used to maintain normal tensile stress perpendicular to the specimen symmetrical axis during the tension. The axial displacement of the specimens was measured using extensometer "Epsilon 676123" with gauge length of 25 mm (Fig. 2).

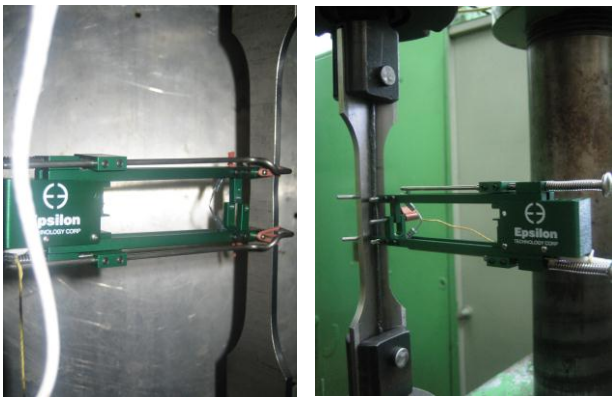

a b

Fig. 2 Strain gauge mounting on the flat (a) and the welded (b) specimen

Before the testing, the load measure elastic element connected with the upper specimen clamping grip by the rigid joint. The testing machine was calibrated using a standard force transducer DOSM 5-1, which is applied for testing machine calibration in the range of 0 – 50 kN. The strain gauge was calibrated using a micrometre-calliper MI-25 with a resolution accuracy of 0.001 mm. The measurements via an oscilloscope "Picoscope 3204 PC Oscilloscope" were recorded by a computer.

The photos of the specimens after fracture are showed in Fig. 3-4.

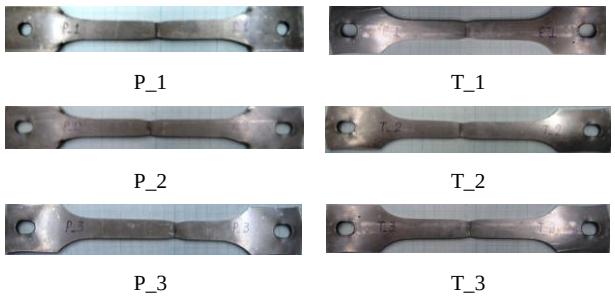

Fig. 3 Photos of the flat specimens (series P) and the tube contoured specimens (series T) after fracture

Fig. 4 Photos of the flat welded specimens (series PW) and the welded tube contoured specimens (series TW) after fracture

Averaged experimental and engineering tensile test curves for all four types specimens are showed in Figs. 5 and 6.

The engineering curves were developed dividing applied force by actual cross-section of the specimen. For this reason, the cross-section of each specimen was calculated as an average of three measurements: on the centre of the specimen working zone and at a distance of ± 25 mm from it. The same procedure was done for the welded specimens, but additionally for them, the weld measures in the same cross-section points were measured as well. These calculations were performed using software "Mechanical Desktop".

Yield stress $R_{p0.2}$, ultimate tensile strength R_m and elongation A_5 of the specimens after break was determined according to the requirements [ISO 6892-1: 2009 and LST EN 10002-1:2003] for each specimen separately and then averaged. Averaged mechanical properties of the stainless 321 steel sheet, tube and HAZ is presented in (Table 2).

Table 2

Averaged mechanical properties of the stainless 321 steel sheet, tube and HAZ

Material, series	Mechanical properties		
	$R_{p0.2}$, MPa	R_m, MPa	A_5, %
Stainless 321 steel, series P	300	603	61.3
Stainless 321 steel, series T	309	606	58.0
Weld + HAZ, series PW	319	623	58.1
Weld + HAZ, series TW	309	593	60.8

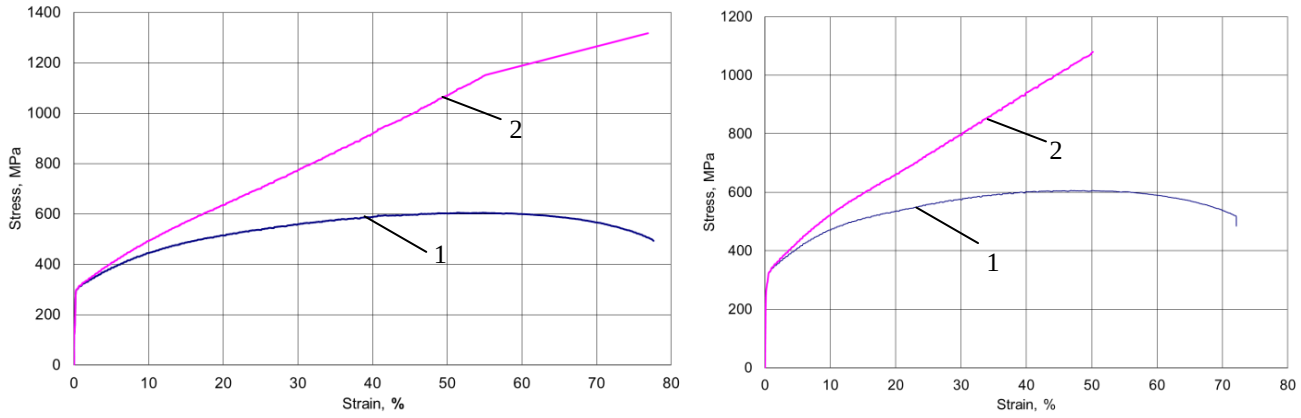

Fig. 5 Averaged engineering and true stress-strain curves for: a – flat specimens; b – tube-contoured specimens; *1* - engineering; *2* - true

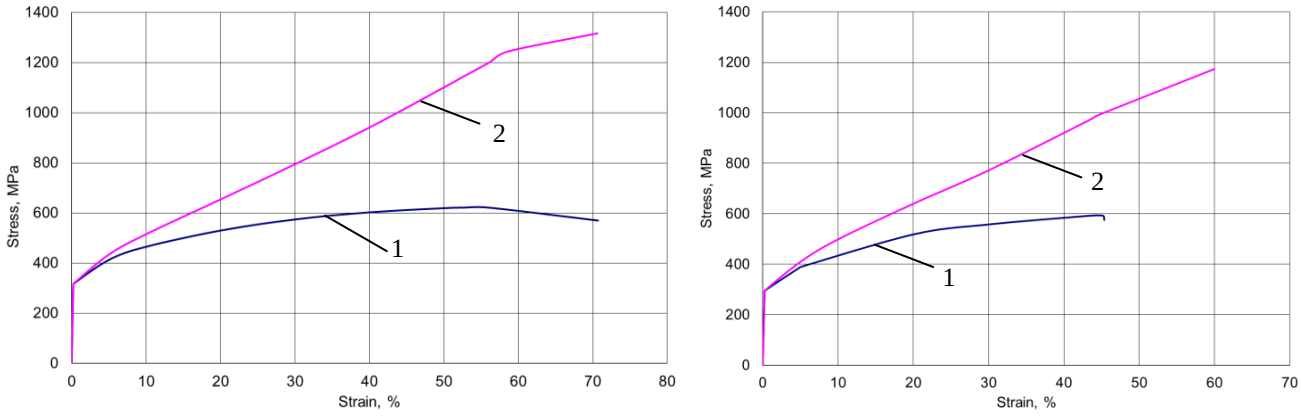

Fig. 6 Averaged engineering and true stress-strain curves for: a – welded flat specimens; b – welded tube-contoured specimens with the longitudinal weld; *1* - engineering; *2* - true

The comparison of the experimental data enabled to conclude that for all, in series tested specimens, the obtained experimental tensile curves were very similar. It means that during plate bending, the material surface becomes hardened, but the internal layers remain plastic, because the difference in this characteristic (elongation) is quite the same.

The welded specimens with the longitudinal welds contain weld metal and a heat affected metal zone, which size depends on welding regimes. Mechanical properties for both types of the specimens $R_{p0.2}$ and R_m varies in a negligible margin and the reason of this variation is weld cross-section variation. So it could be stated, that the electrodes CT36 are selected properly.

4. FEM modelling of pillar strength and a loaded pillar impact on a rigid surface

The purpose of the analysis is to calculate the maximum axial force in compression and to model the behaviour of the pillar, if the pillar with a heavy weight structure mounted on top of it will be dropped from a height of 5 meters.

4.1. Static analysis of pillar compression

Considering predicted design conditions, a tube with a longitudinal weld with a diameter of 400 mm, a wall thickness of 5 mm and a length of 800 mm was modelled as the pillar.

Static analysis of pillar compression was performed using finite element analysis software ABAQUS. The pillar calculation scheme for static load is showed in Fig. 7.

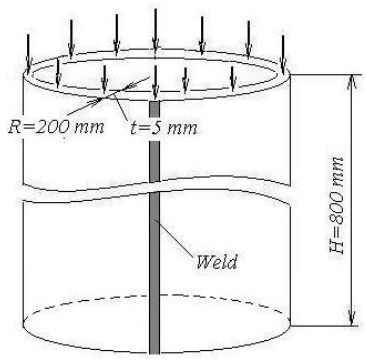

Fig. 7 Pillar calculation scheme for static loading

The isotropic hardening plasticity model was applied to define the tube and weld materials using the obtained true stress-strains curves (Fig. 5, b; Fig. 6, b).

In order to get more accurate results and to save

computational time, the pillar was meshed with an adaptive mesh. C3D4 4-node linear tetrahedron elements were used for meshing. For the remising rule Von Mises stress were selected as the error variable.

The dependency of maximal Von Misses stress $\sigma_{v\,max}$ on the load mass m_l was obtained (Fig. 8). It showed that when the static load reaches about 160 tons, plastic strains in the pillar occur.

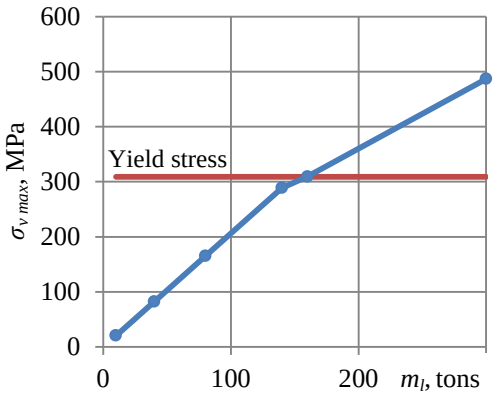

Fig. 8 Dependency of maximal Von Misses stress $\sigma_{v\,max}$ on the static load mass m_l

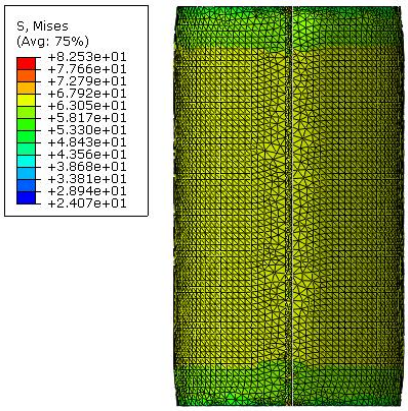

Fig. 9 Distribution of Von Misses stress (MPa) under 40 tons static loading

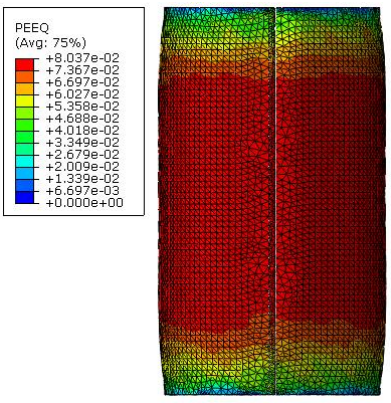

Fig. 10 Distribution of equivalent plastic strain under 300 tons static loading

The distribution of Von Misses stress in the pillar, when the static load is 40 tons, is showed in Fig. 9. The distribution of equivalent plastic strain, when the static load is 300 tons, is showed in Fig. 10.

4.2. Explicit dynamic analysis of a loaded pillar impact on a rigid surface

The modelling of a pillar impact with a load on a rigid surface was performed using finite element analysis software ABAQUS/EXPLICIT. The finite element model geometry (Fig. 11) consists of the pillar with a surface on the top, which is tied to it and acts like the mounted structure, and a surface beneath the pillar.

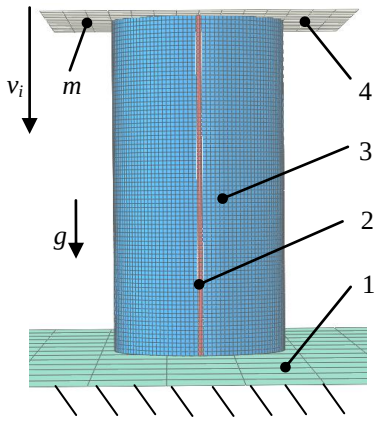

Fig. 11 Mesh and boundary conditions for the impact analysis: *1* – the lower surface on which the pillar falls; *2* – the longitudinal weld of the pillar; *3* – the tube; *4* – the top platform

The mass m_l of the structure mounted on the pillar is assigned to the top surface. Only the longitudinal degree of freedom of this surface is left free while others are restrained. The lower surface is fixed. The higher and lower surfaces are constrained to be rigid. The model simulates the impact of the pillar on the lower surface when the pillar with the mounted structure is dropped from a height of 5 m.

The tube and the weld have been meshed using brick element C3D8R, which has 8-node tri-linear displacement and reduced integration with hourglass control. The adaptive meshing and element deletion techniques were deployed in the model. The surfaces were meshed using 4-node quadrilateral surface elements SFM3D4R with reduced integration. A total of 31005 elements have been generated in the model (Fig. 11).

In order to save computational time, the mass scaling technique was used in the simulation. Mass scaling was performed every 10 increments to obtain a stable time increment of at least 10^{-8} s step time.

In dynamic explicit analysis, the isotropic hardening plasticity model was applied to define tube and weld materials using the obtained true stress-strains curves (Fig. 5, b; Fig. 6, b). The ductile damage initiation criterion was used in this study. The fracture strain value from the true stress-strains curves was used to govern damage initiation.

The initial velocity v_i for the load and the pillar was set to 9.903 m/s, which is the velocity of an object free fall from a height of 5 m without taking into account air resistance. The free fall acceleration g due to gravity was set to 9.806 m/s^2.

Fig. 12 shows how the speed of the mounted structure decreases after the pillar impacts the surface under different masses of the mounted structure (loads). After

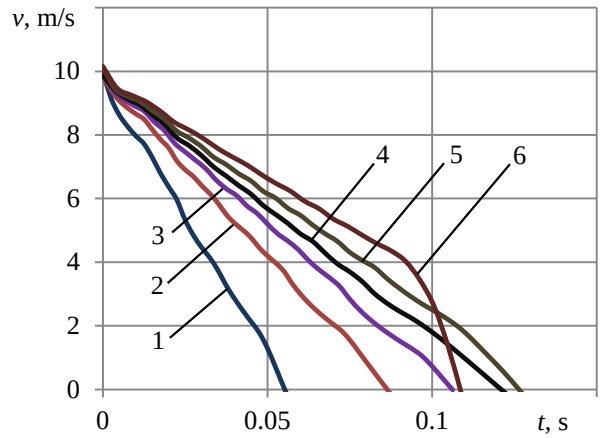

Fig. 12 Speed decrease after the impact under different loads: *1* – 5 tons; *2* – 7.5 tons; *3* – 9 tons; *4* – 10 tons; *5* – 11 tons; *6* – 12.5 tons

the impact on the lower surface, the pillar springs back a little bit from it. The speed variation after the spring back is not showed in this figure. The dynamic simulation showed that the pillar is able smoothly to decrease the speed of the mounted structure after the impact when the weight of the structure is up about to 11 tons. As it seen from the speed variation (Fig. 12, curve *6*) and the deformed pillar shape (Fig. 13, e), when the load is 12.5 tons, the pillar folds completely at about 0.9 s after the impact and after that the speed decreases more rapidly. According to this, the most reasonable load for the pillar is 9 – 11 tons under these impact conditions. The pillar deformed shape (the view from the bottom) after the impact with the equivalent plastic strain distribution when the load is 12.5 tons is showed in Fig. 14. The bottom of the pillar deforms in a triangular shape and three cracks occur in the corners of the triangle. Von Misses stress values reach 1297 MPa in the pillar (Fig. 13).

The simulation showed that the longitudinal weld does not influence an adverse effect, the pillar deforms smoothly without cracks, if it is not overloaded.

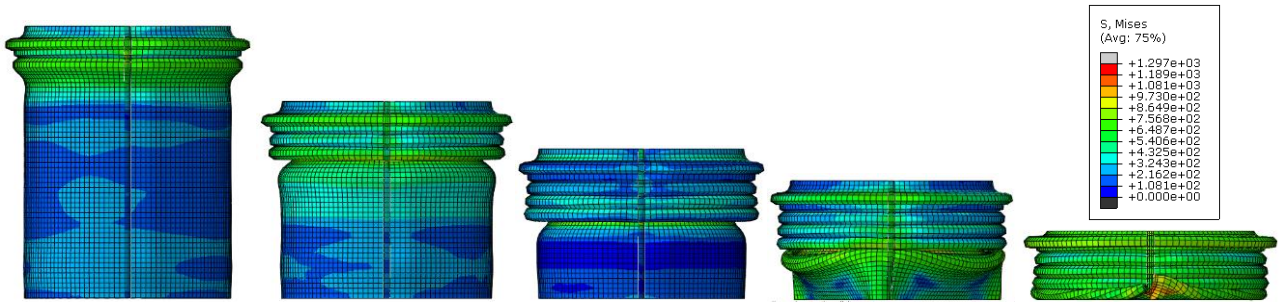

a b c d e

Fig. 13 Von Misses stress distribution (MPa) in the deformed shape of the pillar after the impact under different loads: a – 5 tons; b – 7.5 tons; c – 9 tons; d – 10 tons; e – 12.5 tons

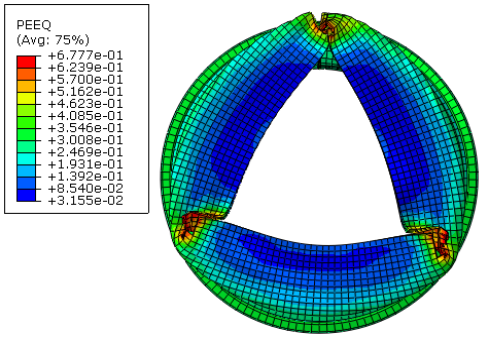

Fig. 14 Pillar deformed shape with the equivalent plastic strain distribution after the impact when the load is 12.5 tons

5. Conclusions

In order to model support pillar behaviour under static and dynamic loading, the influence of manufacture factors on mechanical properties of the pillar steel and its welded joint was examined. For this reason, the standard tensile test using four types of specimens – standard flat, tube contoured and the same ones containing longitudinal weld has been carried out. The comparison of the experimental data enabled to conclude that during plate bending, the material surface becomes hardened, but the internal layers remains plastic, because the difference of this characteristic (elongation) is quite the same and it means, that the welding electrodes were selected properly.

Using the obtained true stress-strain curves, the static analysis of pillar compression in the longitudinal direction was carried out and the simulation of the behaviour of the pillar, if the pillar with a heavy weight structure mounted on top of it will be dropped from a height of 5 meters, was performed.

The static analysis showed that when the static load is 40 tons, the pillar structure satisfies high safety requirements. When the static load reaches about 160 tons, plastic strains in the pillar occurs and the pillar losses its strength.

The dynamic impact simulation showed that the pillar is able smoothly to decrease the speed of the mounted structure after the impact when the weight of the structure is up about to 14 tons. According to the obtained results, the most reasonable load for the pillar is 9 – 11 tons. The simulation showed that the longitudinal weld does not influence an adverse effect, the pillar deforms smoothly without cracks, if it is not overloaded.

References

1. **Allahbakhsh, H.R.; Saemi, J.; Hourali, M.** 2011. Design optimization of square aluminium damage columns with crashworthiness criteria, Mechanika 17(2): 187-192. http://dx.doi.org/10.5755/j01.mech.17.2.338.
2. **Shariati, M.; Allahbakhsh, H.R.; Saemi Jafar** 2010. An experimental and numerical crashworthiness investigation of crash columns assembled by spot-weld, Mechanika 2(82): 21-24.
3. **Zhang, X.; Huh, H.** 2010. Crushing analysis of polygonal columns and angle elements, International Journal of Impact Engineering 37(4): 441-451. http://dx.doi.org/10.1016/j.ijimpeng.2009.06.009.
4. **Shariati, M.; Allahbakhsh, H.R.; Saemi, J.; Sedighi, M.** 2010. Optimization of foam filled spot-welded column for the crashworthiness design, Mechanika 3(83): 10-16.
5. **An, Y.; Wen, C.; Hodgson, P.; Yang, C.** 2012. Impact response and energy absorption of aluminium foam-filled tubes, Applied Mechanics and Materials, Vols. 152–154: 439-439. http://dx.doi.org/10.4028/www.scientific.net/AMM.152-154.436.
6. **Daunys, M.; Krasauskas, P.; Dundulis, R.** 2009. Fracture toughness of 19MN5 steel pipe welded joints materials, Acta Mechanica et Automatica, Bialystok Technical University, 3(4): 24-27.
7. **Daunys, M.; Krasauskas, P.; Dundulis, R.** 2005. Fracture toughness of welded joints materials for main pipelines at Ignalina NPP, Nuclear Engineering and Design 235(7): 747-760. http://dx.doi.org/10.1016/j.nucengdes.2004.10.006.

R. Dundulis, P. Krasauskas, S. Kilikevičius

IŠILGINE SIŪLE SUVIRINTOS ATRAMINĖS KOLONOS STIPRUMO IR PASLANKUMO MODELIAVIMAS BEI IMITAVIMAS

R e z i u m ė

Eksploatuojant krovinių platformas turi būti užtikrintas atraminių konstrukcijų patikimumas ir krovos darbų sauga, todėl jas projektuojant, skaičiuojamieji modeliai turi įvertinti ne tik ribinių statinių apkrovų poveikį, bet ir avarinių situacijų atvejais gebėti atlaikyti bei amortizuoti smūgines apkrovas. Modeliuojant tokių konstrukcijų apkrovas BEM metodais, reikia žinoti tikslias medžiagų mechanines charakteristikas, tačiau jas galima nustatyti tik atliekant standartinius tempimo bandymus, pagaminant tokius bandinius, kurie įgalintų įvertinti konstrukcinius ir technologinius tokių atramų gamybos veiksnius.

Šio darbo tikslas buvo eksperimentiškai nustatyti nerūdijančio plieno 321 lakšto, iš kurio bus gaminamos atramos, vamzdžio ir terminio poveikio zonos metalo mechanines charakteristikas, įvertinti kaip jos pasikeičia po lenkimo operacijos ir vamzdžio suvirinimo. Tuo tikslu iš plieno lakšto buvo pagaminti standartiniai keturių tipų bandiniai: lygūs plokšti, vamzdžio kontūro, kurių spindulys atitinka sulenkto vamzdžio, spindulį, bei analogiški bandiniai, suvirinti išilgine siūle plieno CT 36 elektrodais. Atlikus statinio tempimo bandymus buvo nustatytos plieno ir terminio poveikio zonos metalo su siūle mechaninės charakteristikos, kurios buvo panaudotos kolonos stiprumo skaičiavimui veikiant statinei ir smūginei apkrovai kai kolona, su ant jos pritvirtinta didelio svorio konstrukcija, numetama iš 5 m aukščio. Statinė analizė parodė, kad atraminė kolona su pakankama atsarga atlaiko 40 tonų statinę apkrovą. Dinaminė analizė parodė, kad racionalus kolonos apkrovimas yra 9 - 11 tonų, o suvirinimo siūlė, jei kolonos apkrova neviršija projektinės, neturi neigiamo poveikio ir deformuojasi tolygiai, be plyšių.

R. Dundulis, P. Krasauskas, S. Kilikevičius

MODELLING AND SIMULATION OF STRENGTH AND DAMPING OF THE SUPPORT PILLAR WELDED BY LONGITUDINAL WELD

S u m m a r y

In some fields of industry, such as stowage works, strongly safety assessment should be ensured, so it is important to design constructions, like platforms, which would withstand heavy static loading and, in emergences situations, to withstand the same bulk, dropped from the predicted height, with the ability to damp it. In order to perform a FEM structural analysis of such structure, the accurate material characteristics should be known. For this reason, four types of specimens - standard flat, tube contoured and the same ones containing longitudinal weld, welded in the longitudinal direction using electrodes CT36, were manufactured from a stainless 321 steel sheet and tested in order to define mechanical properties of the material. Using the obtained true stress-strain curves, the static analysis of pillar compression was carried out and the simulation of its behaviour, if a heavy weight structure will be dropped from a height of 5 meters, was performed. The static analysis showed that, when the static load is 40 tons, the pillar structure satisfies high safety requirements. The dynamic impact simulation showed that the most reasonable load for the pillar is 9 - 11 tons and, if it is not overloaded, the longitudinal weld does not influence an adverse effect and the pillar deforms smoothly without cracks.

Keywords: tensile test, damping, impact simulation.

Received June 03, 2011
Accepted April 12, 2012